Chemistry
A European
Journal

Accepted Article

This manuscript has been accepted after peer review and appears as an Accepted Article online prior to editing, proofing, and formal publication of the final Version of Record (VoR). The VoR will be published online in Early View as soon as possible and may be different to this Accepted Article as a result of editing. Readers should obtain the VoR from the journal website shown below when it is published to ensure accuracy of information. The authors are responsible for the content of this Accepted Article.

N-Heterocyclic Carbene Boranes: Dual Reagents for the Synthesis of Gold Nanoparticles

Dr. Laura Hippolyte,[a,b#] *Dr. Omar Sadek,*[b,†#] *Salem Ba Sowid,*[a,b#] *Dr. Alexandre Porcheron,*[a,b] *Dr. Nathalie Bridonneau,*[a,b,†] *Dr. Sébastien Blanchard,*[b] *Prof. Marine Desage-El Murr,*[b] *Dr. David Gatineau,*[c] *Dr. Yves Gimbert,*[c] *Dr. Dimitri Mercier,*[d] *Prof. Philippe Marcus,*[d] *Dr. Clément Chauvier,*[b] *Prof. Corinne Chanéac,*[a] *Dr. François Ribot,*[a]* *Prof. Louis Fensterbank*[b]*

# These authors contributed equally

[a] Sorbonne Université, CNRS, Laboratoire de Chimie de la Matière Condensée de Paris (LCMCP), F-75252 Paris Cedex 05, France
E-mail: francois.ribot@sorbonne-universite.fr ; ORCID: 0000-0001-5576-7725
https://lcmcp.upmc.fr/site/pages-personnelles/francois-ribot/

[b] Sorbonne Université, CNRS, Institut Parisien de Chimie Moléculaire (IPCM), F-75252 Paris Cedex 05, France
E-mail: louis.fensterbank@sorbonne-universite.fr ;   ORCID: 0000-0003-0001-7120
https://www.ipcm.fr/FENSTERBANK-Louis

[c] Département de Chimie Moléculaire (UMR CNRS 5250), Université Grenoble Alpes, F-38050 Grenoble, France
[d] PSL Research University, CNRS – Chimie ParisTech, Institut de Recherche de Chimie Paris (IRCP), Physical Chemistry of Surfaces Research Group, Paris, France

Abstract: *N*-heterocyclic carbenes (NHCs) have drawn considerable interest in the field of nano-materials chemistry as highly stabilizing ligands enabling formation of strong and covalent C-metal bonds. Applied to gold nanoparticles synthesis, the most common strategy consists in the reduction of a preformed NHC-Au(I) complex with a large excess of a reducing agent rendering the particle size difficult to control. In this paper, we report on the straightforward synthesis of NHC-coated gold nanoparticles (NHC-AuNPs) by reacting a commercially-available gold(I) precursor with an easy-to-synthesize NHC-BH_3 reagent. The latter acts as both the reducing agent and the source of surface ligands operating under mild conditions. Mechanistic studies including NMR spectroscopy and mass spectrometry demonstrate that the reduction of gold(I) generates NHC-BH_2Cl as a byproduct. This strategy garners efficient control over the nucleation and growth of gold particles by varying the NHC-borane/gold(I) ratio, allowing unparalleled particle size variation in the range of 4.9 ± 0.9 nm to 10.0 ± 2.7 nm. Our strategy also allows the unprecedented precise and controlled seeded growth of gold nanoparticles. In addition, the as-prepared NHC-AuNPs exhibit narrow size distributions without engaging extensive purification or size selectivity techniques and are stable over months.

1

Introduction

Gold nanoparticles (AuNPs) have attracted interest for many years due to their remarkable properties that have been explored both fundamentally as well as in direct technical applications in various fields such as imaging, medicine, or catalysis.[1-7] As non-stabilized (i.e. "naked") AuNPs tend to aggregate and precipitate as bulk Au(0), strategies to prevent their aggregation and promote their long term stability have been devised. One approach involves covering the AuNPs with capping agents. While thiols are historically the most common, other ligands including phosphines,[8] amines,[9] or carboxylates,[10] have found applications. These protecting ligands can also play an important role in the synthesis of the particles, rendering them compatible with solvents of different polarity,[11] or introducing functional motifs that confer additional properties (luminescence, catalysis),[12] or to promote binding to specific targets of interest.[13]

Among possible capping/surface ligands, *N*-heterocyclic carbenes (NHCs) based on the 1,3-imidazol-2-ylidene scaffold, have emerged as particularly important.[14] They have shown exquisite potential for the stabilization of metallic nanoparticles[15,16] (Ru,[17] Pt,[18] Pd,[19] Ir[20]), including gold,[19,21] due to their facile synthesis,[22] and especially for their strong carbon-metal bond,[23,24] specifically when compared to thiols,[25] or phosphines.[26] The first syntheses of NHC-AuNPs have been inspired by well-known protocols developed for thiol-protected gold nanoparticles (Stucky,[27] Brust[28]). Typically, syntheses consist in either reducing a well-defined, isolated and purified or *in-situ* generated Au(I)-NHC[21a] complex or imidazolium haloaurate salt,[21b] known as the "bottom-up" approach (Scheme 1a). Alternatively, NHC-AuNPs can be accessed by ligand exchange on preformed AuNPs capped with a sacrificial labile ligand, termed the "top-down" approach (Scheme 1b).[19] Our group has also recently established the base-free synthesis of NHC-capped nanoparticles with tunable sizes (6-12 nm) by altering the nature of the reducing agent employed (NaBH$_4$ vs. *t*-BuNH$_2$BH$_3$).[29]

A common feature in all these strategies is the requirement for a reducing agent (usually a borohydride salt) to be added as an exogenous additive. Consequently, in its simplest formulation the reaction medium comprises of the latter reductant and a stabilizing ligand, thereby complexifying the synthetic mixture. We have thus sought a novel approach towards AuNPs synthesis that would only rely on a single molecular precursor that would play a dual role of both reducing agent and source of stabilizing NHC ligand. We surmised that *N*-heterocyclic carbene-borane reagents (NHC-boranes or NHC-BH$_3$) could fulfill such a requirement given they are structurally comprised of a reducing borane moiety and a NHC ligand. NHC-boranes are already known in the literature as bench stable Lewis adducts that are easily synthesized.[30] They have, for instance, been used for the reduction of ketones,[31] organic halides,[32] and xanthates,[33] among others.[34] Recently, we validated the application of NHC-BH$_3$ as a dual reagent for the direct synthesis of copper nanoparticles using mesitylcopper(I) ([CuMes]$_n$) as copper precursor under thermal conditions (refluxing toluene).[35] However, the application of this strategy towards the synthesis of NHC-AuNPs has yet remained unexplored.

Leveraging our group's experience with borane reagents and the synthesis of gold nanoparticles, we report herein the application of NHC-BH₃ as dual reagents for the synthesis of NHC-AuNPs (Scheme 1).
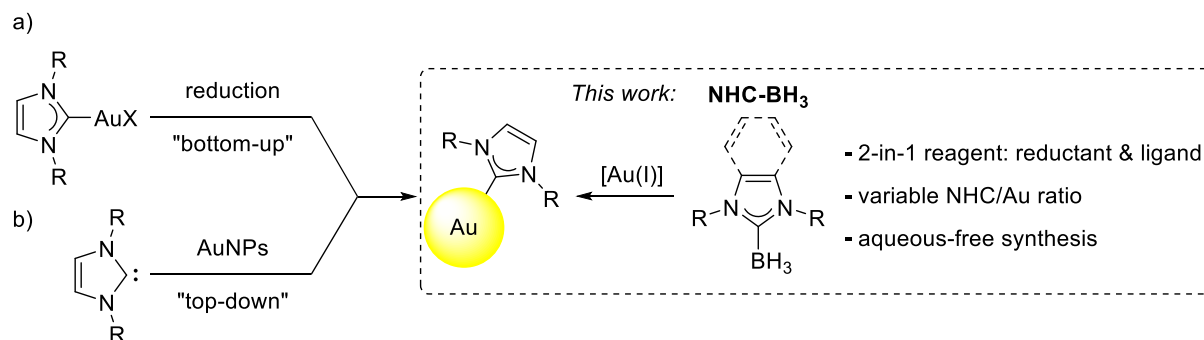

Scheme 1. Synthetic strategies towards AuNPs: a) "bottom-up" approach, b) "top-down" approach and this work using NHC-BH₃.

Results and Discussion

Towards the aim of further optimizing NHC-AuNPs synthesis, and keeping in mind that long alkyl chains promote efficient stabilization of nanoparticles,[21a,29,35,36] we focused on NHC-borane reagent **1**. For this study, the gram-scale preparation of **1** was optimized. Thus, the deprotonation of the bis-$C_{12}H_{25}$ imidazolium bromide salt by KHMDS at -78°C followed by the addition of $BH_3 \cdot THF$ and purification through simple crystallization, provided **1** as a stable white solid in an improved yield of 66% (Scheme 2, top). After screening various Au(I) and Au(III) precursors, a straightforward synthesis of NHC-protected AuNPs was devised. In a typical synthesis, $Me_2S \cdot AuCl$ and **1** were separately dissolved in toluene to obtain 1 mM and 7 mM solutions, respectively. Under ambient conditions, the solution of **1** was added to an equal volume of $Me_2S \cdot AuCl$ and the mixture turned dark red almost instantaneously, signaling the formation of AuNPs (Scheme 2, bottom).
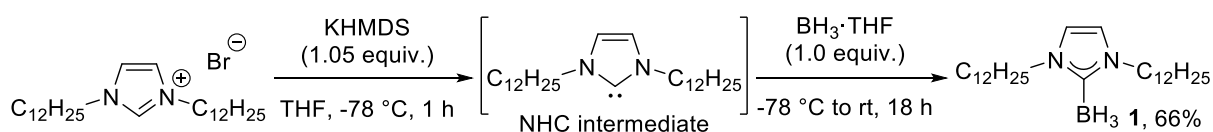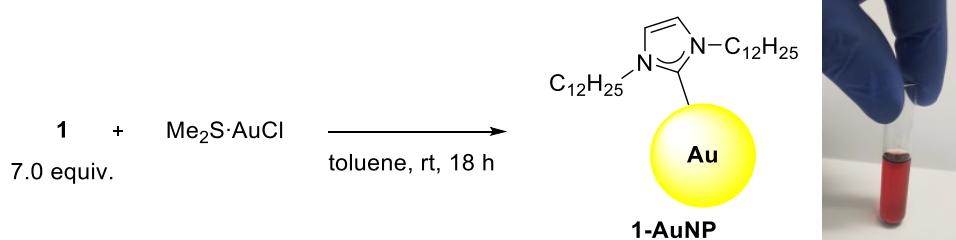
Scheme 2. Synthesis of NHC-BH₃ **1** (top) and synthesis of **1-AuNPs** (bottom).

The obtained AuNPs nanoparticles were directly analyzed from the crude colloidal solution. TEM images revealed that the **1-AuNPs** were rather spherical and monodisperse with a mean diameter of 6.0 ± 1.4 nm, as presented in Figure 1.
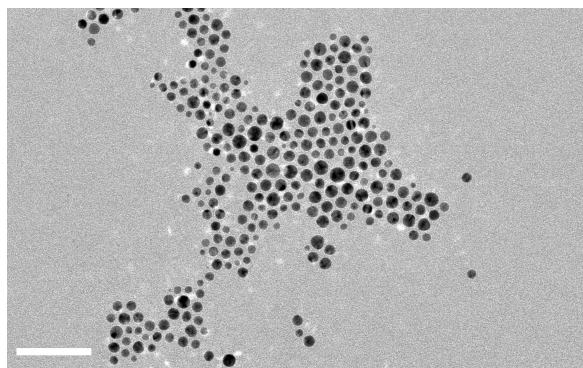

Figure 1. TEM images of NHC-protected gold nanoparticles **1-AuNPs** from a 1:7 Au/NHC-BH$_3$ ratio (mean diameter: 6.0 ± 1.4 nm). Scale bar is 50 nm.

Following the optimization of the reaction conditions, we explored the variation of the NHC-borane to gold(I) ratio, which revealed an important size-dependent effect (see Figures S1-S9). Figure 2 presents the mean nanoparticle diameters for Au/**1** ratios varying from 1:1 to 1:28. The smallest nanoparticles were obtained for Au/**1** ratios lower than 1:7 reaching a minimum of 4.9 ± 0.9 nm for the 1:28 ratio. Increasing the Au/**1** ratio above 1:7 resulted in a sharp increase in particle size. The largest AuNPs were obtained with a 1:1 ratio (10.0 ± 2.7 nm). This was accompanied by a slight decrease in the AuNPs colloidal stability only for the highest ratios (1:2 and 1:1), evidenced by the presence of aggregates along with AuNPs in suspension. The 1:0.5 ratio yielded no dispersed nanoparticles, although immediate reduction occurred as indicated by a color change of the solution from colorless to dark blue. Such a range of variation in a single step synthesis has been rarely reported for NHC stabilized Au-NPs. So far, a "top-down" approach has usually been used to synthesis large NHC-AuNPs.[19] However, it requires the prior synthesis of Au-NPs before the exchange process and might suffer from an incomplete exchange of the ligands.[19c]
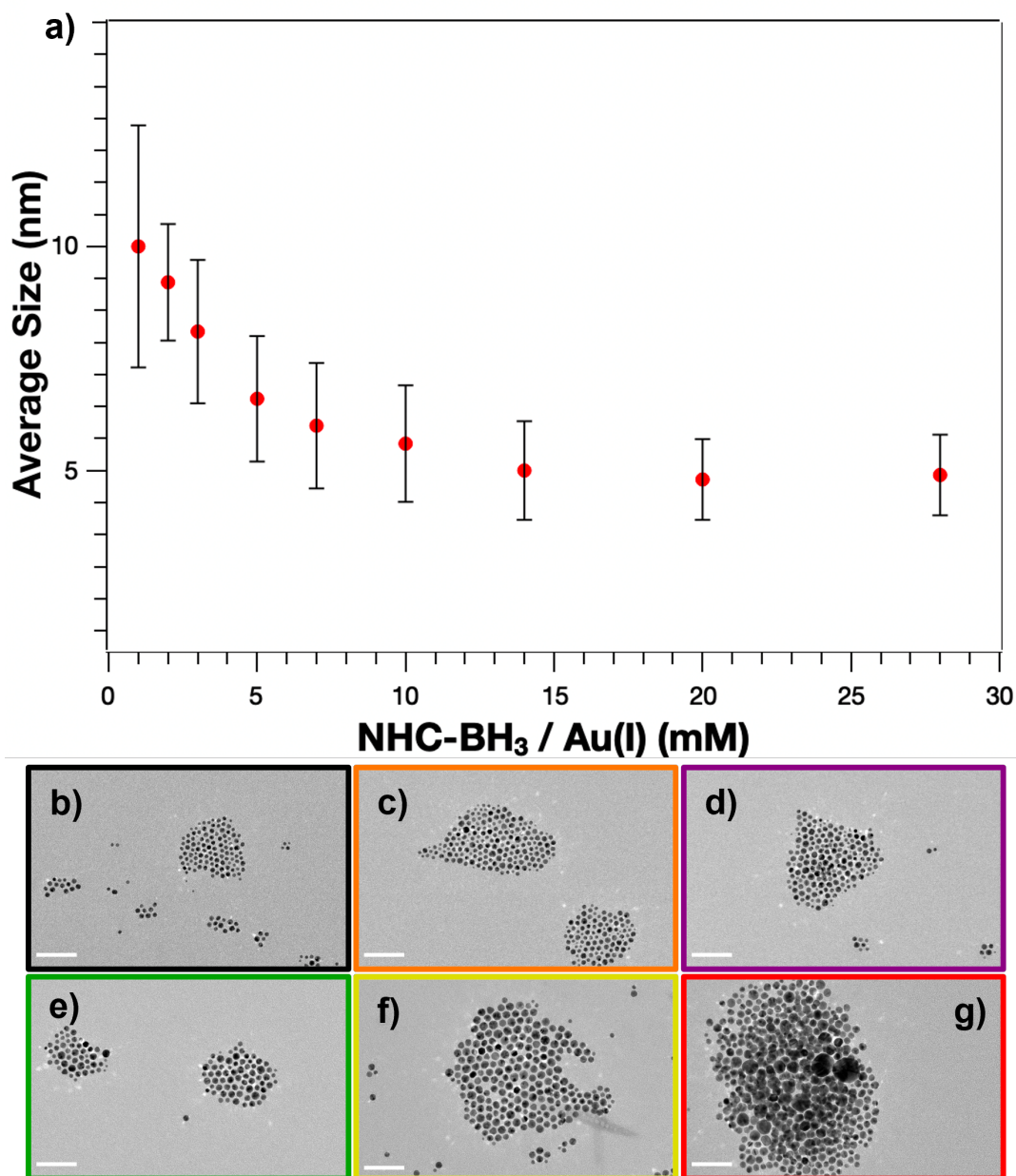
Figure 2. a) Diameter variation of **1-AuNPs** depending on Au:**1** ratio. TEM images of crude solutions of different ratios: b) 1:28 (4.9 ± 0.9 nm), c) 1:14 (5.0 ± 1.1 nm), d) 1:10 (5.6 ± 1.3 nm), e) 1:5 (6.6 ± 1.4 nm), f) 1:3 (8.1 ± 1.6 nm), g) 1:1 (10.0 ± 2.7 nm & aggregates). Scale bars are 50 nm.

Further characterization of the **1-AuNPs** and species in solution was carried out *via* various analytical techniques. Both NHC-borane **1** and the centrifugated and washed nanoparticles (1:7 ratio) were analyzed by X-ray photoelectron spectroscopy (XPS). The general spectrum of **1** showed the presence of carbon, nitrogen, and boron. High-resolution spectra obtained for C1s, N1s and B1s core levels confirmed that **1** possessed the expected composition of the ligand (Table S1). XPS analyses of the gold nanoparticles **1-AuNPs** revealed the presence of carbon, nitrogen, and gold elements (Table S2). Formation of the **1-AuNPs** was demonstrated by the concomitant disappearance of boron on the B1s high resolution spectrum and the presence of metallic gold (84 eV) as a single component, evidencing that

5

the core and surface of the nanoparticles are purely comprised of Au(0). This observation indicates that the NHC-AuNPs prepared from NHC-BH$_3$ are different from those prepared from NHC-AuX complexes, which have been reported to provide mixed valence Au(0)/Au(I) nanoparticles.[37]

The relative ratio of the high-resolution C1s and N1s spectra were once again in accordance with ligand composition hence attesting to ligand integrity on the nanoparticle surface. The N1s photopeak obtained for **1** and the AuNPs are presented in Figure 3, in addition to the N1s photopeak previously reported for the corresponding imidazolium bromide.[29] The binding energy of **1** (400.9 eV) is shifted towards lower energy compared to the imidazolium bromide (401.8 eV) in accordance with the loss of charge on the heterocycle concomitant with imidazolium conversion to an NHC. Concerning the gold nanoparticles **1-AuNPs**, the binding energy is shifted towards even lower energy (400.3 eV). The obtained binding energy is almost identical to the binding energy observed for NHC-capped AuNPs obtained using a previously reported protocol (400.2 eV)[29] or for CuNPs obtained from **1**.[35] This evolution indicates strengthening of carbene coordination moving from a C-B to a C-Au bond. Further evidence for the C-Au bond is provided by the C1s photopeak deconvolution of **1** that has been carried out in light of our previous XPS studies concerning imidazolium bromide and their related gold nanoparticles. These deconvolutions are presented in the SI (see Figures S11 and S12). It is important to note the presence of a component at 286.7 eV corresponding to the C-B bond in **1** (Table S1 and Figure S11). A similar deconvolution was carried out for the AuNPs obtained from **1** (Table S2 and Figure S12), showing once again a component at low energy (283.9 eV) which is characteristic of the C-Au bond. As in previous works,[29] a similar component at high energy (288.5eV) was observed and attributed to the π->π* transition from the photoexcitation of the heterocycle ring. This component, only observed during NPs characterization confirms the hypothesis of an enhancement by the plasmonic effect.
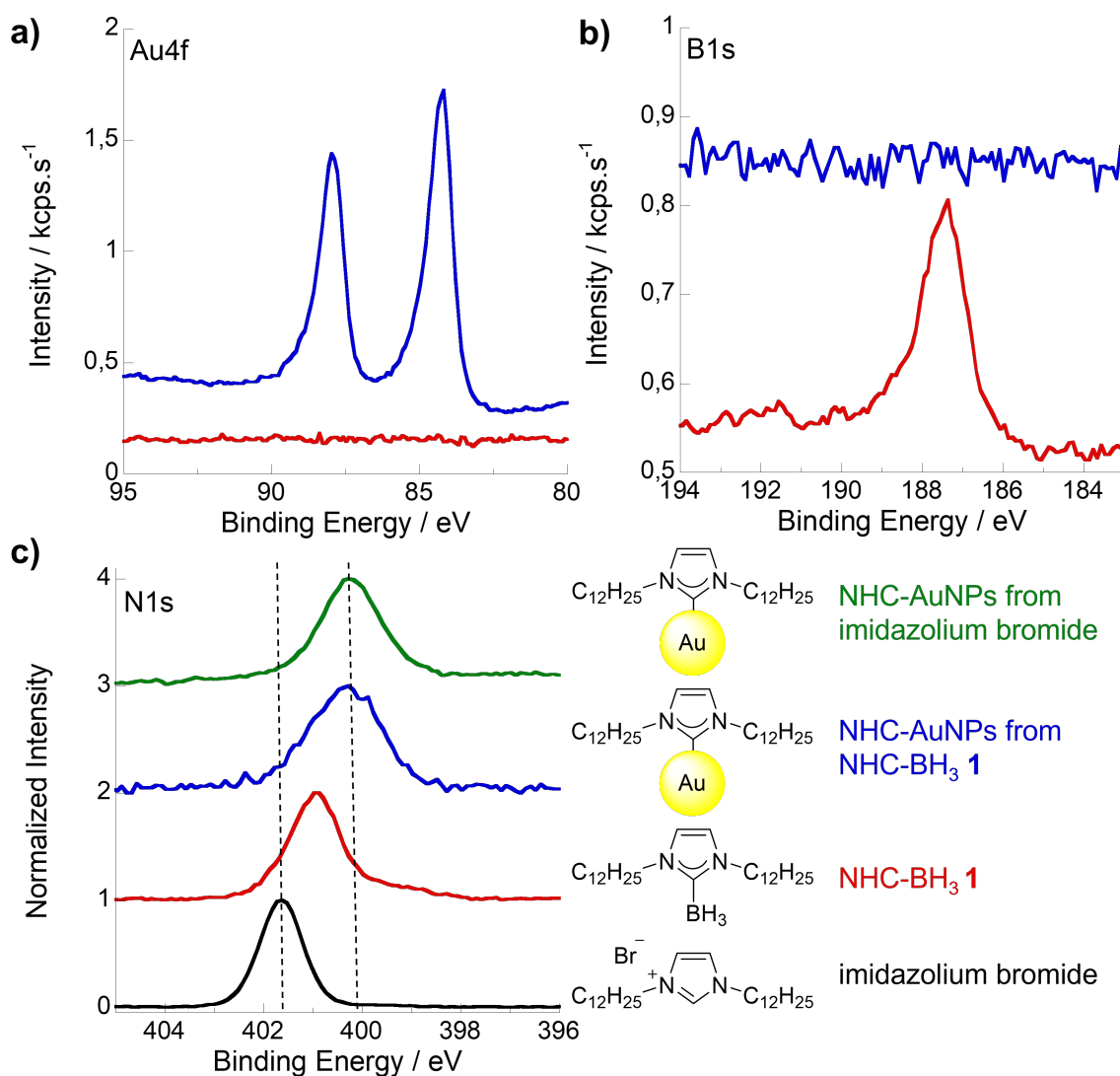
6

WILEY-VCH

Figure 3. High resolution XPS spectra of (a) Au4f and (b) B1s obtained for **1** (red) and **1-AuNPs** (blue); (c) high-resolution N1s photopeaks for imidazolium bromide (black), **1** (red), **1-AuNPs** (blue) and NHC-AuNP using a reported protocol[29] (green).

The centrifugated nanoparticles (1:7 ratio) were also characterized by NMR spectroscopy. ^{11}B NMR spectra further confirmed the absence of boron, however ^{13}C NMR spectra did not allow us to identify the carbon signal of the coordinated carbene. This is likely due to the proximity of the carbene to the gold surface which broadens the signal into the baseline.[17,21a,29,38]

In order to clarify the role of **1** in the reduction of the gold(I) precursor, further NMR spectroscopy experiments were performed in deuterated toluene (Figure 4). Upon mixing $Me_2S \cdot AuCl$ (1 equivalent) with **1** (7 equivalents), while nanoparticles were indeed formed, the majority of the available NHC borane **1** remained in solution and only a small amount of a new species, associated to a ^{1}H NMR signal at 5.90 ppm, appeared (see Figure 4). With a mixture composed of 1 equivalent of $Me_2S \cdot AuCl$ and 1 equivalent of **1**, the relative amount of this new molecular species clearly increased. Decreasing the quantity of **1** to 0.5 equivalent, relative to $Me_2S \cdot AuCl$, resulted in almost complete disappearance of NHC-BH_3 **1**

in favor of this new species. ^{11}B NMR showed a peak at -18.6 ppm (see Figure S14), too broad to evidence any [11]B-^{1}H scalar coupling (^{11}B-{^{1}H} NMR spectrum was as broad), but an additional signal at 3.38 ppm was observed in a ^{1}H-{^{11}B} NMR experiment (see Figure S15). Comparison with an authentic sample,[39] allowed us to identify this new species as NHC-BH_2Cl **2**, which was also confirmed by MS (see Figure S16). Free Me_2S, uncoordinated to gold, was also detected by ^{1}H NMR (see Figure S15).
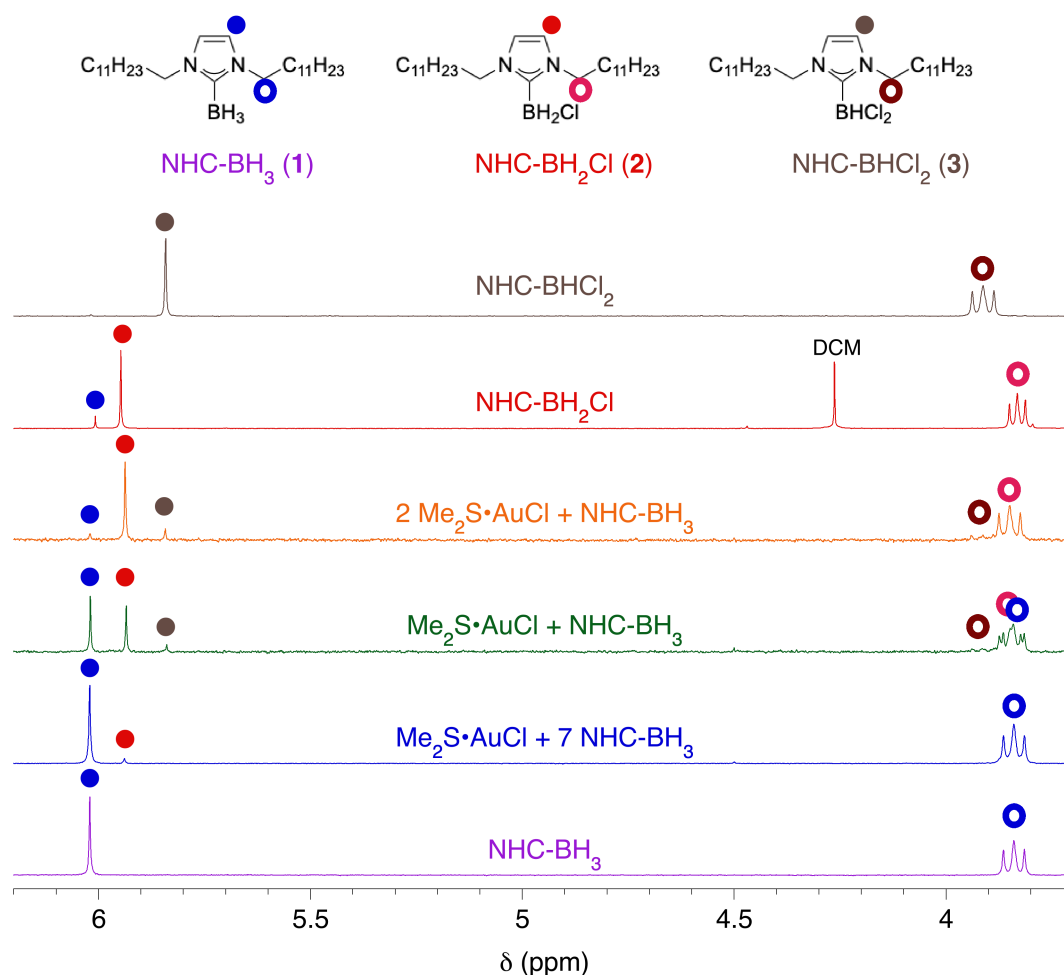
Figure 4. ^{1}H NMR spectroscopy experiments evidencing the formation of NHC-BH_2Cl **2** and the very minor formation of NHC-$BHCl_2$ **3** during the synthesis of **1-AuNPs**.

Importantly, these ^{1}H NMR experiments were performed with an added internal standard, $Si_8O_{12}(OSiMe_3)_8$ (Q^8M^8), whose unique ^{1}H signal is close to 0 ppm. Integrations indicate that no more than 5% of NHC might be consumed during the formation of the AuNPs. From these studies, it appears that the reduction of Au(I) to Au(0) can be achieved with only half of an equivalent of NHC-BH_3 implying the following overall reaction balance:

$$2\ Me_2S\cdot AuCl\ +\ NHC\text{-}BH_3\ \longrightarrow\ 2\ Au\ +\ NHC\text{-}BH_2Cl\ +\ HCl\ +\ 2\ Me_2S$$

8
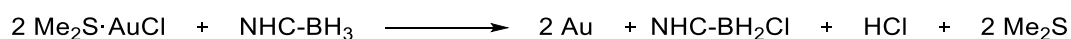
Based on the examination of redox potentials, Au(I)/Au(0) = + 1.83 V (standard potential[40]) and $\mathbf{1}^{+\bullet}/\mathbf{1}$ = 1.06 V *vs* SCE (see Figure S17), direct oxidation of **1** by single electron transfer (SET) could occur yielding Au(0) and the corresponding NHC-BH$_3^{+\bullet}$, the latter undergoing proton loss to generate the NHC-BH$_2^\bullet$ radical (Scheme 3a).[30],[41] This NHC-BH$_2^\bullet$ species could evolve to NHC-BH$_2$Cl (possibly *via* a second SET giving a borenium NHC-BH$_2^+$ intermediate)[42] or by direct reaction with Me$_2$S·AuCl (Scheme 3b). Alternatively, a heterolytic pathway via a gold hydride species AuH cannot be ruled out.[43]
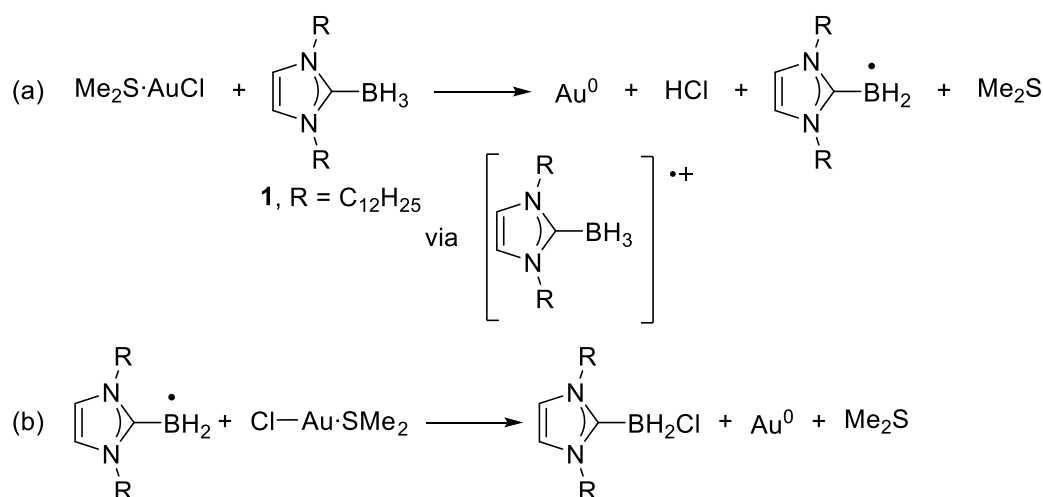
Scheme 3. Potential reduction pathway of Au(I) by **1**.

As the reduction of Au(I) to Au(0) by **1** yields NHC-BH$_2$Cl **2** as byproduct, which still contains hydrides, we questioned whether the latter compound could also reduce Au(I) and participate in the formation of AuNPs. Therefore, 30 minutes after the mixing of 1 equivalent of Me$_2$S·AuCl and 0.5 equivalent of **1**, which, according to ^{1}H NMR, corresponds to the full conversion of **1** into **2** (see Figure 4), another equivalent of Me$_2$S·AuCl was added. This resulted in the very slow growth (over several days) of a ^{1}H signal at 5.84 ppm (See Figures S18-S20). By comparison with an authentic sample,[39] this latter species corresponds to NHC-BHCl$_2$ **3**, which could also be observed as a very minor byproduct during **1-AuNPs** synthesis as seen in Figure 4. The ^{11}B NMR spectrum of **3** reveals a resonance at -6.5 ppm and its ^{1}H-{^{11}B} NMR spectrum displays a singlet at 4.3 ppm, corresponding to the B*H* proton. Therefore, NHC-BH$_2$Cl **2** seems to be able to reduce Au(I), but at a much slower rate than **1**, despite a similar oxidation potential ($\mathbf{2}^{+\bullet}/\mathbf{2}$ = 1.18 V *vs* SCE, Figure S17). Thus, the formation of **1-AuNPs** would primarily result from the reductive reactivity of **1** and not of **2**. Interestingly, if no additional Me$_2$S·AuCl was added, the ^{1}H NMR spectrum of the mixture of 1 equivalent of Me$_2$S·AuCl and 0.5 equivalent of **1** did not further evolve once NHC-BH$_3$ is converted into NHC-BH$_2$Cl (i.e.. after 30 min, see Figure 4). The minor amount of NHC-BHCl$_2$ (**3**) visible at that stage most likely resulted from the action of generated HCl on NHC-BH$_2$Cl[38] and not from the oxidation of NHC-BH$_2$Cl into NHC-BHCl$_2$, which would be very slow. While these studies shed light on the initial reduction steps and formation of Au(0) atoms, which then associate to form gold nanoparticles, we were still curious as to the source of the NHC surface ligands. In that quest, one should note that whatever the source of NHCs, only a

9

small quantity is necessary as surface ligand. Indeed, for **1-AuNPs** with a diameter of 5 nm, only 30% of gold atoms are at the surface. With a surface coverage around 3 NHCs per nm^2,[44] the global NHC/Au ratio is as low as 6%. The NP syntheses being performed with more than two NHC-BH$_3$ per gold, it results that less than 3% of the initial NHC content are to be found on the NP surface.

While the NHC→BH$_3$ interaction is strong, we postulated that the presence of Au(0) might induce ligand exchange from BH$_3$ to Au(0) due to the strength of the NHC→Au(0) interaction (Figure 5). Indeed, after incubating a gold surface in a NHC-BH$_3$ solution (7 mM, toluene) we observed the grafting of NHC ligands onto the metallic surface. This was evidenced by XPS spectroscopy, which revealed a N1s photopeak at 400 eV with the absence of a B1s photopeak (see Figure S13). These results support the possibility that NHC capping ligands could originate from excess NHC-BH$_3$ by NHC ligand exchange from BH$_3$ to the formed Au(0) NPs in solution. Importantly, this finding is highly promising regarding the development of novel self-assembled monolayers (SAMs) techniques on metallic surfaces, due to its facile implementation and clean deposition of surface ligands.
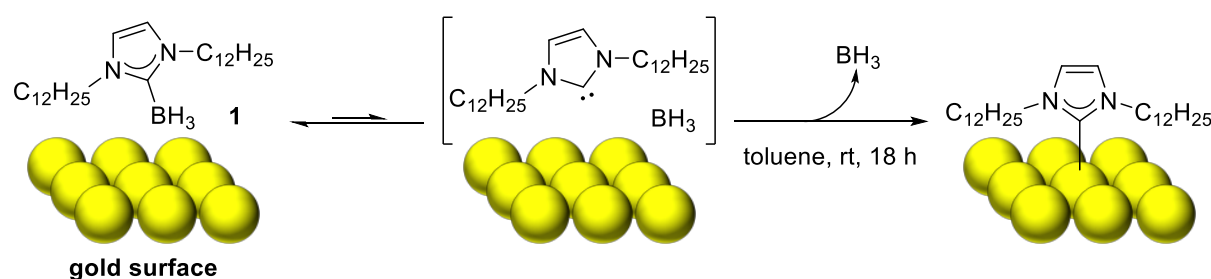
Figure 5. Proposed NHC/BH$_3$ ligand exchange to Au for Au surface functionalization.

To investigate whether the unreacted NHC-BH$_3$, which remains at the end of the syntheses of **1-AuNPs** could still be used to reduce supplementary gold ions, we programmed several subsequent additions of gold(I) precursor to the crude nanoparticle suspension obtained with a Me$_2$S·AuCl to NHC-BH$_3$ ratio of 1:28. Upon the addition of gold precursor to the crude suspension, the red solution became somewhat darker purple/red indicating the reduction of Au(I) to Au(0). UV-Vis analysis (Figure 6) revealed an increase of the plasmonic band after each addition, accompanied by its red shift from 522 nm for the seeds to 531 nm after five successive additions of gold precursor. According to previous literature findings,[45] this observation tends to indicate an increase of the size of the nanoparticles.

10

Figure 6. UV-Vis spectra of the AuNPs seeds, obtained for a Me$_2$S·AuCl:NHC-BH$_3$ ratio of 1:28 and after each subsequent addition of Me$_2$S·AuCl (absorbance is corrected for the dilution associated to the addition of more gold precursor).
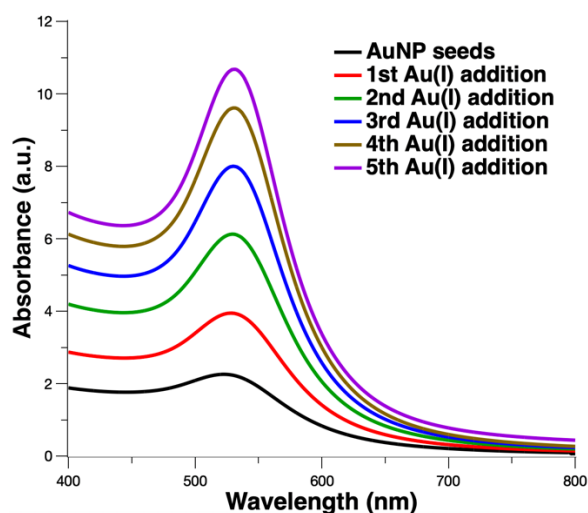
TEM observations (Figure 7 and Table 1) confirm the growth after each successive addition. The seeds, which have a size of 4.8 ± 0.8 nm, finally reach 7.7 ± 1.0 nm after five additions. With the assumption that all the Au(I) introduced is reduced to Au(0), the number of nanoparticles after each addition can be calculated from the observed average size and the total amount of gold introduced (+2 μmoles for each addition). These values are reported in Table 1. After the first addition (sample B), the number of AuNPs increases (+50%), which tends to indicate the occurrence of a second nucleation. Yet, as it does not double, growth of the seeds must also take place, at least to some extent. On the contrary, after the second addition (sample C), the number of **1-AuNPs** appears slightly reduced (-5%), which indicates growth associated to a marginal redistribution of the matter contained in the smaller particles (i.e. ripening). For the three subsequent additions (sample D, E and F), the number of particles remains constant, in line with a clean growth phase. All these results evidence that unreacted **1** can be further engaged in the production of **1-AuNPs** if further Au(I) is added. Moreover, with this process, the growth of NHC-stabilized AuNPs can be achieved, an unprecedented finding in AuNPs synthesis.
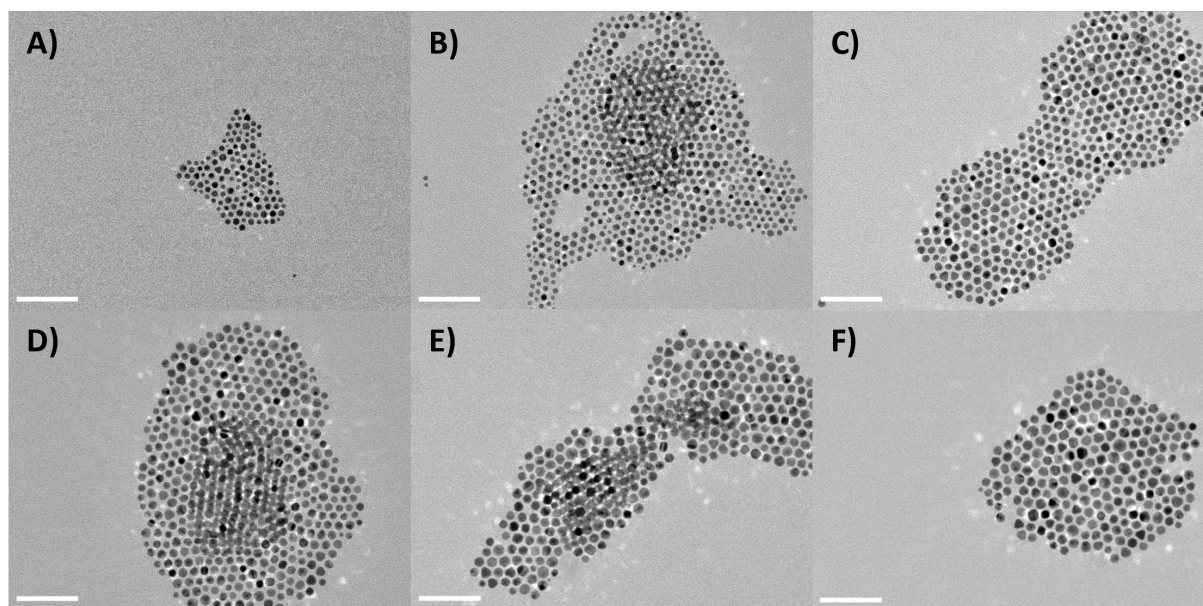
11

Figure 7. TEM images of the AuNPs seeds (A), obtained for a $Me_2S \cdot AuCl$:NHC-BH_3 ratio of 1:28 and after each subsequent addition of $Me_2S \cdot AuCl$ (B to F). Scale bars are 50 nm.

Table 1. Sizes (nm), plasmon band maximum (nm) and calculated number of Au NP for the seeds (A), obtained for a $Me_2S \cdot AuCl$:NHC-BH_3 ratio of 1:28, and after each subsequent addition of $Me_2S \cdot AuCl$ (B to F).

Samples	Size ± SD[a]	Plasmon band maximum[b]	Number of Au NP[c]
AuNPs seeds (A)	4.8 ± 0.8	522	$3.5 \cdot 10^{14}$
1st Au(I) addition (B)	5.3 ± 0.8	529	$5.2 \cdot 10^{14}$
2nd Au(I) addition (C)	6.2 ± 1.0	529	$4.9 \cdot 10^{14}$
3rd Au(I) addition (D)	6.8 ± 1.1	530	$5.0 \cdot 10^{14}$
4th Au(I) addition (E)	7.3 ± 1.0	531	$5.0 \cdot 10^{14}$
5th Au(I) addition (F)	7.7 ± 1.0	531	$5.1 \cdot 10^{14}$

[a] Average size and standard deviation, as determined by TEM image analysis; [b] determined from UV-Vis spectra (in toluene); [c] calculated from the average size and the total amount of gold atoms ($1.20 \cdot 10^{18}$, $2.41 \cdot 10^{18}$, $3.61 \cdot 10^{18}$, $4.82 \cdot 10^{18}$, $6.03 \cdot 10^{18}$ and $7.23 \cdot 10^{18}$ for A, B, C, D, E and F, respectively), see SI Section 7 for the detail of the calculation.

Finally, we showed that the use of 2-in-1 NHC-boranes for the preparation of AuNPs is not specific to **1**. To this end, we prepared the benzimidazolium-derived reagent **1-F** and demonstrated that the corresponding **1-F-AuNPs** were formed upon reaction with $Me_2S \cdot AuCl$ (Scheme 4, see Figure S10).
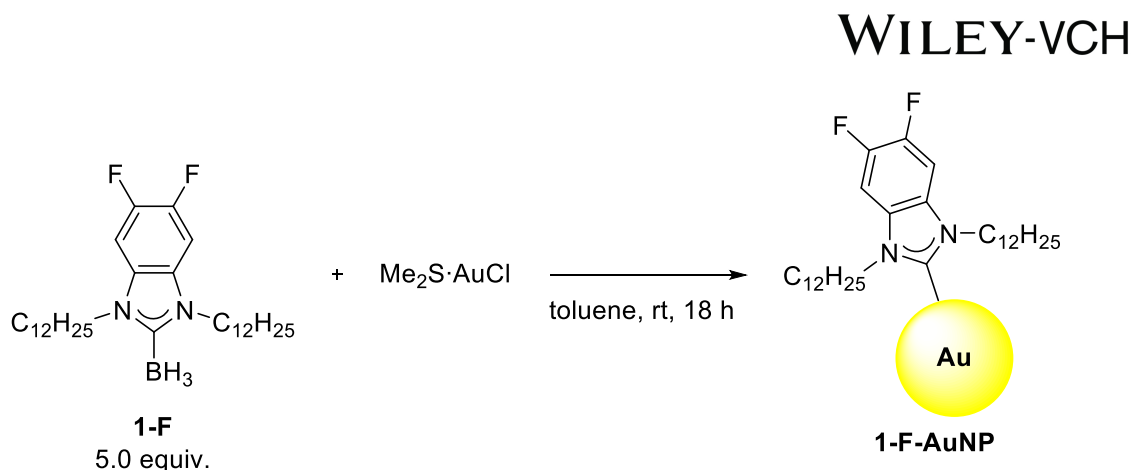
Scheme 4. Synthesis of nanoparticles **1-F-AuNPs** from NHC-borane **1-F**.

Conclusion

The application of NHC-boranes as bench stable dual reagents, acting both as reducing agents and surface ligand precursor, allows the synthesis and stabilization of gold nanoparticles. The procedure for nanoparticle synthesis is exceedingly simple, involving a homogenous one-step protocol only requiring the mixing of the NHC-borane with $Me_2S \cdot AuCl$, used as gold(I) precursor, under mild conditions. Importantly, this method avoids the need for NHC-Au(I/III) complex synthesis and the use of exogenous reducing agents. It also allows the synthesis of stable NHC-AuNPs, which present narrow size distributions without engaging any purification or size selectivity techniques and whose size can be simply controlled by the Au/ligand ratio over a range very rarely reported so far (5-10 nm). Moreover, these NHC-boranes unlock the possibility for a seeded growth process. Our process can be exploited to allow the precisely controlled growth of preformed nanoparticles, a previously unknown strategy with NHC stabilized gold nanoparticles.

Thus, we demonstrate that NHC-boranes are effective dual reagents for the synthesis of NHC-AuNPs with tuned sizes. This simple protocol will allow access to new possibilities regarding nanoparticles synthesis, due to the facile preparation of NHC-borane reagents. It could enable AuNP surface functionalization with more elaborate and complex ligands which may be incompatible with classic AuNP syntheses. Finally, even if the NHC-BH_3 must be prepared first, as are the NHC-Au(I) complexes or imidazolium haloaurate salts, it can then be engaged in the synthesis of other metallic nanoparticles, as already demonstrated with copper.

Experimental Section/Methods

General Information:

Solvents and Reagents

All reactions were performed in oven-dried glassware under air, or an argon atmosphere as stated. Dry solvents were obtained as follows: 1) CH_2Cl_2 was dried over CaH_2 and collected by distillation, 2) THF was distilled from sodium benzophenone ketyl. Other solvents used were commercial grade and used as received with no drying unless otherwise noted. All chemicals were purchased from commercial sources and used as received unless otherwise stated. For $BH_3 \cdot THF$ solution (1 M in THF) the quality and purity of the reagent was assessed by ^{11}B NMR prior to use. 1,3-didodecylimidazolium bromide was prepared according to a reported protocol.[35] Deuterated solvents for NMR spectroscopic analysis were purchased from Eurisotop.

Analyses

NMR experiments were performed in deuterated solvents. ^{1}H, ^{13}C and ^{11}B NMR spectra were recorded on Avance 300, 400 or 600 MHz Bruker spectrometers. All spectra were recorded at ambient temperature (300 K). Chemical shifts (δ) are reported in parts per million (ppm) relative to the residual protium in the solvents (^{1}H) or the solvent signal (^{13}C) as internal standards. External $BF_3 \cdot OEt_2$ was used as reference for ^{11}B NMR. Multiplicity of signals is indicated using the following abbreviations: s (singlet), b (broad), d (doublet), dd (doublet of doublet), t (triplet), q (quadruplet), p (pentet) and m (multiplet).

Reactions were monitored using Merck Silica gel 60 F254 aluminum backed plates. TLC plates were visualized by UV fluorescence (λ= 254, 365 nm) and $KMnO_4$ stain. Flash column chromatography was performed using Sigma-Aldrich Silica gel 60 – 200 μm.

Nanoparticle purification was performed by centrifugation using a Sigma high speed centrifuge (3-30KS) equipped with a 12150-H rotor.

High-resolution mass spectra (HRMS) were recorded on a micrOTOF Bruker with an ESI or APCI source.

UV/Vis spectra were collected using an Agilent Cary 5000 UV-Vis-NIR spectrometer using quartz cuvettes with a 10 mm path length. Samples were dissolved in toluene.

Transmission electron microscopy (TEM) samples were prepared by dropping colloidal suspensions onto a copper grid coated with a carbon film and allowing the solvent to evaporate in air. The TEM images were obtained using a Tecnai Spirit G2 microscope operating at 120 kV. Size distribution histograms were obtained by measuring at least 500 particles per sample using the ImageJ software.

14

X-ray photoelectron spectroscopy (XPS) spectra were recorded with a Thermo ESCALAB 250Xi X-ray photoelectron spectrometer with a monochromatic Al-Kα X-Ray source (hν = 1486.6 eV) operating at 10^{-10} Torr. The analyzer pass energy was 100 eV for the survey spectra and 20 eV for the high-resolution spectra. All spectra were calibrated versus the binding energy (BE) of hydrocarbons (C 1s at 285.0 eV). Spectra were recorded and analyzed using the Thermo Avantage software. For curve fitting and decomposition, a Shirley-type background subtraction has been used and the shape of fitting curves was obtained by a 70% Gaussian/30% Lorentzian distribution.

X-ray crystallography. A single crystal of the compound was selected and mounted onto a glass fiber. Intensity data were collected with a BRUKER Kappa-APEXII diffractometer with Mo-Kα radiation (λ=0.71073 A) at room temperature (ca 295K). CELL_NOW(BRUKER) was used to determine the orientation matrices of the two domains. APEX 4 suite and SAINT program (BRUKER) were used to carry out data collection, unit-cell parameters refinement, integration and data reduction. TWINABS (BRUKER) was used for scaling and multi-scan absorption corrections. In the Olex2 suite,[47] the structure was solved with SHELXT-14[48] program and refined by full-matrix least-squares methods using SHELXL-14[49] firstly an HKLF4 file and secondly a HKLF5 file. All non-hydrogen atoms were refined anisotropically. H atoms were mostly placed at calculated positions except for those on boron atom which were located from Fourier difference map. Deposition Number <url href="https://www.ccdc.cam.ac.uk/services/structures?id=doi:10.1002/chem.202301610">2252912 (for **1-F**)</url> contains the supplementary crystallographic data for this paper. These data are provided free of charge by the joint Cambridge Crystallographic Data Centre and Fachinformationszentrum Karlsruhe <url href="http://www.ccdc.cam.ac.uk/structures">Access Structures service</url>.

Synthetic Procedures:

NHC-BH₃ 1

A 100 mL round-bottom flask was charged with a stir bar and 1,3-didodecylimidazolium bromide (2.39 g, 4.9 mmol), the imidazolium was dried under vacuum at 60 °C for 6 hours. After cooling to room temperature, the flask was purged with argon, and THF (24 mL) was added; the mixture was stirred to completely dissolve all solids. The flask was then cooled to -78 °C, using an acetone/N₂ bath, after which potassium bis(trimethylsilyl)amide (KHMDS, 1.05 eq., 1 M in THF, 5.2 mL, 5.2 mmol) was added dropwise to the stirring reaction mixture. The mixture was stirred at -78 °C for 1 hour, after which BH₃·THF (1.0 eq. ~0.75 M in THF, 6.6 mL, 4.9 mmol) was added dropwise to the stirring reaction mixture. The cooling bath was removed, and the reaction mixture allowed to slowly warm to room temperature overnight. Volatiles were then removed under reduced pressure. The remaining residue was dissolved in CH₂Cl₂ and filtered over Celite®; the filtrate was concentrated under reduced pressure to furnish a yellow oil.

<u>NOTE</u>: purification of this product <u>must be performed by crystallization</u>; purification via silica gel column chromatography[35] leads to irreproducible results regarding NHC-AuNP synthesis.

The NHC-BH$_3$ was purified by crystallization from CH$_2$Cl$_2$/pentane, in a vessel of appropriate volume, by dissolving the residue in a minimum of CH$_2$Cl$_2$ and carefully layering the CH$_2$Cl$_2$ solution with an excess of pentane (≥ 10-fold volume of CH$_2$Cl$_2$). The crystallization vessel was placed in a -18 °C freezer overnight, which resulted in the formation of a white crystalline precipitate. The precipitate was collected by filtration and washed with cold (0 °C) pentane. The filtrate (mother liquor) was recovered, and all volatiles removed under reduced pressure and the recovered residue was submitted to another round of purification by crystallization. Both crops gave pure NHC-BH$_3$ as a white crystalline powder with a combined yield of 1.36 g (66%). Spectroscopic data matches those previously reported.[35] IR v_{max}/cm^{-1} (neat film): 3171, 3138, 3123, 2954, 2918, 2849, 2329, 2282, 1667, 1572, 1561, 1471, 1458, 1430, 1375, 1238, 1217, 1130. ^{1}H NMR (600 MHz, CDCl$_3$, δ): 6.79 (s, 2H), 4.08 (t, $^3J_{H-H}$ = 7.6 Hz, 4H), 1.76 (p, $^3J_{H-H}$ = 7.6 Hz, 2H), 1.36 – 1.19 (m, 36H), 1.02 (s, 3H, BH$_3$), 0.87 (t, $^3J_{H-H}$ = 7.0 Hz, 6H). The BH$_3$ protons were observed through a ^{1}H{^{11}B} NMR experiment. ^{13}C NMR (101 MHz, CDCl$_3$) δ 171.8 ($C_{carbene}$-BH$_3$), 118.8, 48.9, 32.1, 30.3, 29.8, 29.77, 29.76, 29.6, 29.5, 29.3, 26.7, 22.8, 14.3. The carbene carbon was observed through a ^{1}H-^{13}C HMBC NMR experiment. ^{11}B NMR (193 MHz, CDCl$_3$, δ): -37.3 (q, $^1J_{B-H}$ = 86.7 Hz).

NHC-BH$_3$ 1-F

Adapting similar protocols,[46],[29] 1,3-didodecyl-5,6-difluorobenzimidazolium bromide (0.35 g, 0.6 mmol), 3 mL THF, potassium bis(trimethylsilyl)amide (KHMDS, 1.05 eq., 1 M in THF, 0.63 mL, 0.63 mmol), BH$_3$·THF (1.0 eq. 1 M in THF, 0.6 mL, 0.6 mmol), After purification by crystallization from CH$_2$Cl$_2$/pentane, the product was obtained as a white crystalline powder (167 mg, 55%). IR v_{max}/cm^{-1} (neat film): 3050, 2954, 2918, 2852, 2323, 2290, 2223, 1618, 1497, 1465, 1415, 1395, 1351, 1250, 1167, 1134, 1118. ^{1}H NMR (400 MHz, CD$_2$Cl$_2$, δ): 7.28 (t, $^3J_{H-F}$ = 8.1 Hz, 2H), 4.33 (t, $^3J_{H-H}$ = 7.5 Hz, 4H), 1.81 (p, $^3J_{H-H}$ = 7.5 Hz, 4H), 1.43 – 1.20 (m, 36H), 1.1 (s, 3H, BH_3), 0.88 (t, $^3J_{H-H}$ = 8.5 Hz, 6H). The BH$_3$ protons were observed through a ^{1}H{^{11}B} NMR experiment. ^{13}C NMR (75 MHz, CD$_2$Cl$_2$, δ): 183.4, 148.5, 128.5, 100.0, 46.5, 32.3, 29.94, 29.88, 29.74, 29.65, 29.2, 27.1, 23.1, 20.0, 14.3. The C$_{Carbene}$-BH$_3$ signal was observed through ^{1}H-^{13}C HMBC NMR experiment. ^{11}B NMR (128 MHz, CD$_2$Cl$_2$, δ): -35.59 (q, $^1J_{B-H}$ = 87.3 Hz). ^{19}F NMR (376 MHz, CD$_2$Cl$_2$, δ): -141.54 (t, $^3J_{F-H}$ = 8.1 Hz). HRMS (ESI) m/z: [M+Na]$^+$ calc'd for C$_{31}$H$_{55}$N$_2$F$_2$BNa 527.4319, found 527.4310. Single crystals were grown by layering a saturated CH$_2$Cl$_2$ solution of **1-F** with cold (0 °C) pentane and storing overnight at -18 °C. A X-ray diffraction analysis of **1-F** was obtained (CCDC 2252912, see SI section 9).

NHC-BH$_2$Cl 2

Following a literature procedure,[39] NHC-borane **1** (0.11 g, 0.26 mmol) was dissolved in freshly distilled CH$_2$Cl$_2$ (0.1 M) before the dropwise addition of dry HCl (1.0 M in Et$_2$O, 1 eq., 0.26 mL) under argon. The solution was stirred for 1 hour at room temperature. The solvent was evaporated providing **2** (113 mg, 96%) along with traces of imidazolium impurities. The

16

product **2** tends to degrade, as the quantity of imidazolium impurity continually increased upon storage. An attempt to isolate **2** pure by silica gel column chromatography was unsuccessful due to its instability towards silica gel. IR v_{max}/cm^{-1} (neat film): 3168, 3144, 3119, 3055, 2954, 2917, 2849, 2408, 2342, 1572, 1499, 1472, 1458, 1434, 1373, 1219, 1217, 1192, 1131, 1107, 1072, 1044. ^{1}H NMR (400 MHz, Tol. d-8, δ): 6.05 (s, 2H), 3.89 (t, $^3J_{H-H}$ = 7.7 Hz, 4H), 1.57 (p, $^3J_{H-H}$ = 7.6 Hz, 4H), 1.43 – 1.05 (m, 36H), 3.37 (s, 1H, BH$_2$Cl), 0.92 (t, $^3J_{H-H}$ = 6.6 Hz, 6H). The BH$_2$Cl proton was observed through a ^{1}H{^{11}B} NMR experiment. ^{13}C NMR (75 MHz, Tol. d-8, δ): 165.8, 118.8, 48.5, 32.1, 30.5, 29.9, 29.8, 29.7, 29.62, 29.56, 29.3, 26.4, 22.8, 14.0. The C$_{Carbene}$-BH$_2$Cl signal was observed through ^{1}H-^{13}C HMBC NMR experiment. ^{11}B NMR (96 MHz, Tol. d-8, δ): -18.09 (bs).

NHC-BHCl$_2$ 3

During an attempt to synthesize **2** using 2 eq. of HCl following the reported protocol,[39] NHC·BHCl$_2$ **3** was rapidly formed instead. NHC-borane **1** (0.11 g, 0.26 mmol) was dissolved in freshly distilled CH$_2$Cl$_2$ (0.1 M) before the addition of dry HCl (4 M in dioxane, 2 eq., 0.13 mL) under argon. The solution was stirred for 3 hours at room temperature. The compound was purified by silica gel chromatography giving **3** as a white solid (37 mg, 29%). IR v_{max}/cm^{-1} (neat film): 3168, 3131, 3116, 2956, 2914, 2852, 2489, 1572, 1472, 1457, 1431, 1374, 1262, 1241, 1173, 1112, 1092, 1019. ^{1}H NMR (300 MHz, Tol. d-8, δ): 5.89 (s, 2H), 3.93 (t, $^3J_{H-H}$ = 7.7 Hz, 4H), 1.53 (p, $^3J_{H-H}$ = 7.6 Hz, 4H), 1.43 – 1.20 (m, 36H), 4.62 (s, 1H, BHCl$_2$), 0.92 (t, $^3J_{H-H}$ = 6.4 Hz, 6H). The BHCl$_2$ proton was observed through a ^{1}H{^{11}B} NMR experiment. ^{13}C NMR (75 MHz, Tol. d-8, δ): 159.8, 119.8, 49.2, 31.0, 32.5, 30.2, 30.1, 30.0, 29.6, 26.7, 23.2, 14.5. The C$_{Carbene}$-BHCl$_2$ signal was observed through ^{1}H-^{13}C HMBC NMR experiment. ^{11}B NMR (96 MHz, Tol. d-8, δ): -6.53 (bs).

General protocol for 1-AuNPs

A 1 mM solution of Me$_2$S·AuCl in toluene is prepared, referred to as [Au]. In parallel, a xx mM (1 to 28 mM) solution of NHC-BH$_3$ **1** in toluene is prepared, referred to as [NHC-BH$_3$]. This allows control of the Au/NHC-BH$_3$ ratio from 1:1 to 1:28. The reaction vial is charged with 2 mL of the [Au] solution, to this an equal volume (2 mL) of the xx mM [NHC-BH$_3$] is added in one portion using a syringe and needle. Upon addition of [NHC-BH$_3$] onto [Au] the homogenous colorless solution immediately turns dark red/burgundy indicating the formation of AuNPs. The mixture is allowed to stand at room temperature for 18 hours. Samples for UV/Vis and TEM analysis are then taken from the crude reaction mixture. For purification, the mixture is concentrated to ~2 mL under reduced pressure and divided (~1 mL/tube) into two centrifuge tubes (Thermo Scientific, Oak Ridge Centrifuge Nalgene™ Tube, PPCO, 3119-0050). The NHC-AuNPs are precipitated with EtOH (~50 mL/tube) and the tubes centrifuged at 19,000 rpm (33902 RCF) for 45 minutes. The supernatant is decanted, and the NHC-AuNP pellets are dispersed in a minimum of toluene (~1 mL/tube) and reprecipitated with EtOH (~50 mL/tube) and centrifuged at 21,000 rpm (414155 RCF) for 1 hour. The supernatant is decanted and the NHC-AuNPs dispersed in a minimum of toluene for storage.

17

WILEY-VCH

General protocol for seeds growth

A 1 mM solution of Me$_2$S·AuCl in toluene (2 mL) is added in one portion using a syringe and needle to the crude nanoparticle suspension **1-AuNPs** obtained with a Me$_2$S·AuCl:NHC-BH$_3$ ratio of 1:28. The mixture was allowed to stand at room temperature and was monitored by UV-Vis spectroscopy until the plasmonic band position and intensity stabilized and stopped evolving. At that point, one drop of the crude solution was taken for TEM analysis. The same procedure was repeated four more times by adding 2 mL aliquots of 1 mM Me$_2$S·AuCl solution each time to the same suspension.

Present Addresses

†Université Paris-Saclay, CNRS, Institut de Chimie Moléculaire et des Matériaux d'Orsay (ICMMO), F-91400 Orsay Cedex, France.

Author Contributions

LH, OS, SBS, AP, NB, DG conducted the synthesis of ligands and nanoparticles, as well as mechanistic studies and TEM studies. XPS studies were performed by DM and PM. SB conducted the cyclic voltammetry studies. ssNMR spectroscopic studies were conducted by FR. MDEM, YG, CChauvier and CChanéac co-supervised the work. FR and LF supervised the work and wrote the paper, in collaboration with OS.

Supporting Information

Supporting Information is available from the Wiley Online Library.

Acknowledgements

References

[1]   C. Louis and O. Pluchery, Eds., *Gold Nanoparticles for Physics, Chemistry and Biology*, World Scientific (Europe) **2017**.

[2]   D. Astruc, F. Lu, J. R. Aranzaes, *Angew. Chem. Int. Ed.* **2005**, *44*, 7852–7872.

[3]   G. A. Somorjai, A. M. Contreras, M. Montano, R. M. Rioux, *Proc. Natl. Acad. Sci.* **2006**, *103*, 10577–10583.

[4]   M. C. Daniel, D. Astruc, *Chem. Rev.* **2004**, *104*, 293–346.

[5]   W. J. Stark, P. R. Stoessel, W. Wohlleben, A. Hafner, *Chem. Soc. Rev.* **2015**, *44*, 5793–5805.

18

WILEY-VCH

[6]   E. C. Dreaden, A. M. Alkilany, X. Huang, C. J. Murphy, M. A. El-Sayed, *Chem. Soc. Rev.* **2012**, *41*, 2740–2779.

[7]   M. J. Mitchell, M. M. Billingsley, R. M. Haley, M. E. Wechsler, N. A. Peppas, R. Langer, *Nat. Rev. Drug Discov.* **2021**, *20*, 101–124.

[8]   J. M. Pettibone, J. W. Hudgens, *ACS Nano* **2011**, *5*, 2989–3002.

[9]   D. V. Leff, L. Brandt, J. R. Heath, *Langmuir* **1996**, *12*, 4723–4730.

[10]   J. Turkevich, P. C. Stevenson, J. Hillier, *Discuss. Faraday Soc.* **1951**, *11*, 55.

[11]   M. J. MacLeod, J. A. Johnson, *J. Am. Chem. Soc.* **2015**, *137*, 7974–7977.

[12]   a) S. Comby, T. Gunnlaugsson, *ACS Nano* **2011**, *5*, 7184-7197; b) C. Eisen, J.M. Chin, M.R. Reithofer, *Chem. Asian J.* **2021**, *16*, 3026-3037.

[13]   P. R. Rauta, P. M. Hallur, A. Chaubey, *Sci. Rep.* **2018**, *8*, 2893.

[14]   M. N. Hopkinson, C. Richter, M. Schedler, F. Glorius, *Nature* **2014**, *510*, 485–496.

[15]   A. V Zhukhovitskiy, M. J. MacLeod, J. A. Johnson, *Chem. Rev.* **2015**, *115*, 11503–11532.

[16]   C. A. Smith, M. R. Narouz, P. A. Lummis, I. Singh, A. Nazemi, C.-H. Li, C. M. Crudden, *Chem. Rev.* **2019**, *119*, 4986–5056.

[17]   P. Lara, O. Rivada-Wheelaghan, S. Conejero, R. Poteau, K. Philippot, B. Chaudret, *Angew. Chem. Int. Ed.* **2011**, *50*, 12080–12084.

[18]   P. Lara, A. Suárez, V. Collière, K. Philippot, B. Chaudret, *ChemCatChem* **2014**, *6*, 87–90.

[19]   a) E. C. Hurst, K. Wilson, I. J. S. Fairlamb, V. Chechik, *New J. Chem.* **2009**, *33*, 1837; b) A. Ferry, K. Schaepe, P. Tegeder, C. Richter, K. M. Chepiga, B. J. Ravoo, F. Glorius, *ACS Catal.* **2015**, *5*, 5414–5420; c) R. W. Y. Man, C.-H. Li, M. W. A. MacLean, O. V. Zenkina, M. T. Zamora, L. N. Saunders, A. Rousina-Webb, M. Nambo, C. M. Crudden, *J. Am. Chem. Soc.* **2018**, *140*, 1576–1579; d) L. Zhang, Z. Wei, S. Thanneeru, M. Meng, M. Kruzyk, G. Ung, B. Liu, J. He, *Angew. Chemie Int. Ed.* **2019**, *58*, 15834–15840; e) J. F. DeJesus, L. M. Sherman, D. J. Yohannan, J. C. Becca, S. L. Strausser, L. F. P. Karger, L. Jensen, D. M. Jenkins, J. P. Camden, *Angew. Chemie Int. Ed.* **2020**, *59*, 7585–7590.

[20]   J. D. Scholten, G. Ebeling, J. Dupont, *Dalt. Trans.* **2007**, 5554.

[21]   a) J. Vignolle, T. D. Tilley, *Chem. Commun.* **2009**, 7230; b) C. J. Serpell, J. Cookson, A. L. Thompson, C. M. Brown, P. D. Beer, *Dalt. Trans.* **2013**, *42*, 1385–1393; c) X. Ling, S. Roland, M. P. Pileni, *Chem. Mater.* **2015**, *27*, 414–423; d) K. Salorinne, R. W. Y. Man, C.-H. Li, M. Taki, M. Nambo, C. M. Crudden, *Angew. Chem. Int. Ed.* **2017**, *56*, 6198–6202.

[22]   a) C. M. Crudden, D. P. Allen, *Coord. Chem. Rev.* **2004**, *248*, 2247–2273; b) F. E. Hahn, M. C. Jahnke, *Angew. Chem. Int. Ed.* **2008**, *47*, 3122–3172.

[23]   a) J. C. Y. Lin, R. T. W. Huang, C. S. Lee, A. Bhattacharyya, W. S. Hwang, I. J. B. Lin, *Chem. Rev.* **2009**, *109*, 3561–3598; b) C. M. Crudden, J. H. Horton, I. I. Ebralidze, O. V Zenkina, A. B. McLean, B. Drevniok, Z. She, H. Kraatz, N. J. Mosey, T. Seki, E. C. Keske, J. D. Leake, A. Rousina-Webb, G. Wu, *Nat. Chem.* **2014**, *6*, 409–414; c) C. M. Crudden, J. H. Horton, M. R. Narouz, Z. Li, C. A. Smith, K. Munro, C. J. Baddeley, C. R. Larrea, B. Drevniok, B. Thanabalasingam, A. B. McLean, O. V. Zenkina, I. I. Ebralidze, Z. She, H.-B. Kraatz, N. J. Mosey, L. N. Saunders, A. Yagi, *Nat. Commun.* **2016**, *7*, 12654; d) L. M. Sherman, S. L. Strausser, R. K. Borsari, D. M. Jenkins, J. P. Camden, *Langmuir* **2021**, *37*, 5864–5871; e) J. L. Peltier, M. Soleilhavoup, D. Martin, R. Jazzar, G. Bertrand, *J. Am. Chem. Soc.* **2020**, *142*, 16479–16485; f)

19

WILEY-VCH

H. Shen, G. Tian, Z. Xu, L. Wang, Q. Wu, Y. Zhang, B. K. Teo, N. Zheng, *Coord. Chem. Rev.* **2022**, *458*, 214425; h) M. Koy, P. Bellotti, M. Das, F. Glorius, *Nat. Catal.* **2021**, *4*, 352–363.

[24]   Cyclic(alkyl)(amino)carbene (CAAC) ligands have also shown promising properties: A. Bakker, M. Freitag, E. Kolodzeiski, P. Bellotti, A. Timmer, J. Ren, B. Schulze Lammers, D. Moock, H. W. Roesky, H. Mönig, S. Amirjalayer, H. Fuchs, F. Glorius, *Angew. Chem. Int. Ed.* **2020**, *59*, 13643–13646.

[25]   R. G. Nuzzo, L. H. Dubois, D. L. Allara, *J. Am. Chem. Soc.* **1990**, *112*, 558–569.

[26]   P. Pyykkö, N. Runeberg, *Chem. – An Asian J.* **2006**, *1*, 623–628.

[27]   N. Zheng, J. Fan, G. D. Stucky, *J. Am. Chem. Soc.* **2006**, *128*, 6550–6551.

[28]   M. Brust, M. Walker, D. Bethell, D. J. Schiffrin, R. Whyman, *J. Chem. Soc., Chem. Commun.* **1994**, 801–802.

[29]   N. Bridonneau, L. Hippolyte, D. Mercier, D. Portehault, M. Desage-El Murr, P. Marcus, L. Fensterbank, C. Chanéac, F. Ribot, *Dalton Trans.* **2018**, *47*, 6850–6859.

[30]   S.-H. Ueng, A. Solovyev, X. Yuan, S. J. Geib, L. Fensterbank, E. Lacôte, M. Malacria, M. Newcomb, J. C. Walton, D. P. Curran, *J. Am. Chem. Soc.* **2009**, *131*, 11256–11262.

[31]   D. M. Lindsay, D. McArthur, *Chem. Commun.* **2010**, *46*, 2474.

[32]   Q. Chu, M. Makhlouf Brahmi, A. Solovyev, S.-H. Ueng, D. P. Curran, M. Malacria, L. Fensterbank, E. Lacôte, *Chem. - A Eur. J.* **2009**, *15*, 12937–12940.

[33]   S.-H. Ueng, M. Makhlouf Brahmi, E. Derat, L. Fensterbank, E. Lacote, M. Malacria, D. P. Curran, *J. Am. Chem. Soc.* **2008**, *130*, 10082–10083.

[34]   D. P. Curran, A. Solovyev, M. Makhlouf Brahmi, L. Fensterbank, M. Malacria, E. Lacôte, *Angew. Chem. Int. Ed.* **2011**, *50*, 10294–10317.

[35]   X. Frogneux, L. Hippolyte, D. Mercier, D. Portehault, C. Chanéac, C. Sanchez, P. Marcus, F. Ribot, L. Fensterbank, S. Carenco, *Chem. – A Eur. J.* **2019**, *25*, 11481–11485.

[36]   C. Richter, K. Schaepe, F. Glorius, B. J. Ravoo, *Chem. Commun.* **2014**, *50*, 3204.

[37]   a) R. Ye, A. V. Zhukhovitskiy, R. V. Kazantsev, S. C. Fakra, B. B. Wickemeyer, F. D. Toste, G. A. Somorjai, *J. Am. Chem. Soc.* **2018**, *140*, 4144–4149; b) A. J. Young, M. Sauer, G. M. D. M. Rubio, A. Sato, A. Foelske, C. J. Serpell, J. M. Chin, M. R. Reithofer, *Nanoscale* **2019**, *11*, 8327–8333; c) S. R. Thomas, W. Yang, D. J. Morgan, T. E. Davies, J. J. Li, R. A. Fischer, J. Huang, N. Dimitratos, A. Casini, *Chem. – A Eur. J.* **2022**, *28*, e202201575.

[38]   C. Goldmann, F. Ribot, L. F. Peiretti, P. Quaino, F. Tielens, C. Sanchez, C. Chanéac, D. Portehault, *Small* **2017**, *13*, 1604028.

[39]   A. Solovyev, Q. Chu, S. Geib, L. Fensterbank, M. Malacria, E. Lacôte, D. P. Curran, *J. Am. Chem. Soc.* **2010**, *132*, 15072-15080.

[40]   A. J. Bard, R. Parsons, J. Jordan, *Standard Potentials in Aqueous Solution*, Marcel Dekker Inc, New York USA **1985**.

[41]   a) J. Qi, F. Zhang, J. Jin, Q. Zhao, B. Li, L. Liu, Y. Wang, *Angew. Chem. Int. Ed.* **2020**, *59*, 12876–12884; b) G. Li, G. Huang, R. Sun, D. P. Curran, W. Dai, *Org. Lett.* **2021**, *23*, 4353-4357.

[42]   M.-A. Tehfe, M. Makhlouf Brahmi, J.-P.Fouassier, D. P. Curran, M. Malacria, L. Fensterbank, E. Lacôte, J. Lalevée, *Macromolecules* **2010**, *43*, 2261-2267.

[43]   H. Ito, T. Saito, T. Miyahara, C. Zhong, M. Sawamura, *Organometallics* **2009**, *28*, 4829-4840.

WILEY-VCH

[44]   H.-K. Kim, A. S. Hyla, P. Winget, H. Li, C. M. Wyss, A. J. Jordan, F. A. Larrain, J. P. Sadighi, C. Fuentes-Hernandez, B. Kippelen, J.-L. Brédas, S. Barlow, S. R. Marder, *Chem. Mater.* **2017**, *29*, 3403–3411.

[45]   a) W. Haiss, N. T. K. Thanh, J. Aveyard, D. G. Fernig*, Anal. Chem.* **2007**, *79*, 4215-4221; b) C. Goldmann, C. Moretti, B. Malher, B. Abécassis, M. Impéror-Clerc, B. Pansu, *Chem. Commun*. **2021**, *57*, 12512–12515.

[46]   H. Shen, X. Tang, Q. Wu, Y. Zhang, C. Ma, Z. Xu, B. K. Teo, N. Zheng, *ACS Nanosci. Au* **2022**, *2*, 520–526.

[47]   O. V. Dolomanov, L. J. Bourhis, R. J. Gildea, J. A. K. Howard, H. Puschmann, *J. Appl. Cryst.* **2009**, *42*, 339–341.

[48]   G. M. Sheldrick, *Acta Crystallographica Section A* **2015**, *71*, 3–8.

[49]   G. M. Sheldrick, *Acta Crystallographica Section C* **2015**, *71*, 3–8.

Twitter

@dimitri_mercier
@lcmcp_paris
@IPCM_Sorbonne

21

NHC-boranes are demonstrated to be efficient dual reagents, as both reducing agent and source of surface ligands, for the synthesis of NHC-coated gold nanoparticles. This strategy allows the synthesis of spherical and monodisperse AuNPs of variable sizes by adjusting the gold to NHC-borane ratio. The NHC-boranes can also be exploited in a seeded growth process, a strategy never before reported with NHC stabilized gold nanoparticles. The protocol is simple, operating under mild conditions and avoids the use of extensive purification methods.

NHC-borane: 2-in-1 Reagent for AuNP Synthesis

reducing agent & surface ligand provider

✔ one-pot, facile synthesis, mild conditions

✔ spherical & monodisperse AuNPs

✔ no extensive purification or size selectivity

✔ variable AuNP size: 4.8 ± 0.9 nm to 10.0 ± 2.7 nm

✔ controlled & precise seeded growth of AuNPs

22